Erschienen in: Conference record of the Thirty-First IEEE Photovoltaic Specialists Conference - 2005 : Coronado Springs Resort, Lake Buena Vista, FL, January 3 - 7, 2005. - Piscataway, NJ : IEEE Operations Center, 2005. - S. 1035-1038. - ISBN 0-7803-8707-4
https://dx.doi.org/10.1109/PVSC.2005.1488310

KINETICS OF HYDROGENATION AND INTERACTION WITH OXYGEN IN CRYSTALLINE SILICON

G. Hahn[1], D. Karg[2], A. Schönecker[3], A.R. Burgers[3], R. Ginige[4], K. Cherkaoui[4],
[1] University of Konstanz, Department of Physics, 78457 Konstanz, Germany
[2] Institute of Applied Physics, University of Erlangen, Staudtstr. 7, 91058 Erlangen, Germany
[3] ECN Solar Energy, PO Box 1, 1755ZG Petten, Netherlands
[4] NMRC, Lee Maltings, Prospect Row, Cork, Ireland

ABSTRACT

Sufficient passivation of recombination active defects in the bulk of crystalline silicon solar cells using atomic hydrogen is a key feature for reaching high conversion efficiencies. This is of special interest for promising low-cost multi-crystalline (mc) materials, as a substantial cost reduction concerning Watt-peak(W_p)-costs seems to be possible. The effectiveness of this hydrogenation is strongly influenced by the diffusion kinetics of atomic hydrogen in silicon. Oxygen impurities seem to play a major role, as they have the ability to trap hydrogen, slowing down the diffusion of hydrogen atoms.

For two crystalline silicon materials the influence of different oxygen concentrations on hydrogen kinetics is discussed. We demonstrate that not only the overall oxygen concentration, but as well the thermal history of the samples has to be taken into account. Precipitation of oxygen alters the diffusion kinetics and has an influence on vacancy concentration. Faster passivation of crystal defects can be reached in low-oxygen samples.

INTRODUCTION

The diffusion of hydrogen in mono Si was extensively studied in the past. Van Wieringen and Warmoltz [1] could determine the diffusivity of H in mono Si, and this data was confirmed to be valid in a broad temperature range (see [2,3] for a summary). Diffusion of hydrogen in mc Si is much more complex because of the additional interaction with defects and not much is known about the kinetics, although mc Si solar cell processing relies a lot on hydrogenation during solar processing to increase efficiency.

Based on results already presented earlier [4,5], this presentation will address some of the remaining issues in the hydrogenation process. This is a key feature for fabrication of efficient solar cells made from defect-rich but cost-effective materials allowing a reduction in W_p-costs.

In this paper two studies will be presented. Both differ in the materials chosen for the experiment. The first experiment was carried out on Ribbon Growth on Substrate (RGS) silicon. This material offers the possibility of a significant cost reduction in photovoltaics because of the very high production speed of 1 wafer per second [6]. As this material contains a large amount of defects, hydrogenation is an important part of the solar cell process to increase material quality. Knowledge on hydrogen kinetics is therefore very important in order to optimise cell processing [7].

On the other hand we have chosen mono-crystalline Czochralski (Cz) silicon with oxygen as the only major contaminant. The lack of other defects in significant concentrations makes Cz an ideal candidate to monitor the effect of oxygen on hydrogen kinetics.

EXPERIMENT

Material 1 - RGS

RGS wafers chosen for this study (p-type, 1 Ωcm) differ only in their oxygen concentration due to modifications in the crystallisation ambient. Other defect concentrations ([C], grain size, dislocation density, etc.) remain constant (see table 1). Sample RGS 2 has the same overall [O] as RGS 1, but due to O-precipitation directly after crystallisation at temperatures >1000 °C for 1 h the interstitial oxygen concentration [O_i] is lower (measured by Fourier-transformed infrared spectroscopy, FTIR). The String Ribbon (SR, 3 Ωcm) sample was chosen as a reference representing low [O] material.

Table 1: Samples used in the first experiment with [O], [C] from SIMS measurements, as-grown [O_i] from FTIR. No calibration between both methods has been applied.

Material	[O] [cm^{-3}]	[O_i] [cm^{-3}]	[C] [cm^{-3}]
RGS1	$3\text{-}4\cdot10^{18}$	$2.9\cdot10^{18}$	$2\text{-}3\cdot10^{18}$
RGS2	$3\text{-}4\cdot10^{18}$	$<10^{18}$	$2\text{-}3\cdot10^{18}$
RGS3	$2\cdot10^{18}$	$0.75\cdot10^{18}$	$2\text{-}3\cdot10^{18}$
RGS4	$0.7\cdot10^{18}$	$0.3\cdot10^{18}$	$2\text{-}3\cdot10^{18}$
SR	$0.2\cdot10^{18}$	$<10^{17}$	$4\cdot10^{17}$

Material 2 - Cz

Whereas in RGS a lot of crystal defects can interact with atomic hydrogen, mono-crystalline Cz material (p-type, 8-13 Ωcm) has been chosen to investigate the effect of oxygen alone on hydrogen kinetics in a second experiment. Two types of Cz with different [O] have been

Konstanzer Online-Publikations-System (KOPS)
URL: http://nbn-resolving.de/urn:nbn:de:bsz:352-2-s6h9tdunqnqz6

used. Whereas Cz1 shows a higher [O] of about $1.7x10^{18}$ cm^{-3}, Cz2 contains less oxygen ([O] = $1.0x10^{18}$ cm^{-3}, table 2).

Both Cz materials have been split into three groups and have been submitted to an initial short homogenisation step at 1050 °C for 15 min. Whereas the first group was then left in this ‘as-grown’ state (after homogenisation), the second and third one were afterwards submitted to additional thermal annealing steps to intentionally create O-precipitates of defined sizes. The annealing steps are visualized in figure 1. Anneal 1 with temperatures of 500 and 650 °C respectively forms small precipitates, whereas during Anneal 2 at 1000 °C larger precipitates are formed.

From table 2 it can be concluded that for the high [O] material Cz1 most oxygen has been precipitated after Anneal 1 and 2, whereas most oxygen remained at interstitial sites for the as-grown sample after the homogenisation step. In Cz2 the lower [O] limits O-precipitation. Only a small fraction of the overall [O] is precipitated. SIMS (secondary ion mass spectroscopy) data for Cz2 samples and the SOLSIX reference (no homogenisation step) are limited due to problems during measurement.

Table 2: [O_i] and [O] data determined by FTIR and SIMS for the samples investigated in this study after high temperature annealing steps. The effect of annealing on O-precipitation can clearly be seen.

Material	[O_i] FTIR [10^{17} cm^{-3}]	[O] SIMS [10^{17} cm^{-3}]
Cz1 as grown	13.8	16.2
Cz1 Anneal 1	2.0	16.4
Cz1 Anneal 2	3.1	17.6
Cz2 as grown	7.2	~9
Cz2 Anneal 1	6.9	
Cz2 Anneal 2	6.0	9.9
mc SOLSIX as grown	~3	~4

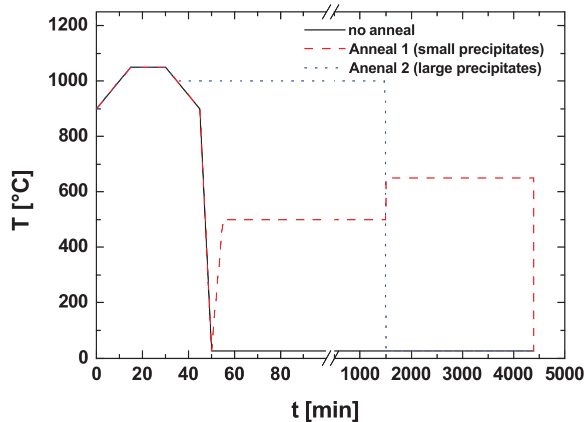

Figure 1: Annealing steps performed for the two Cz materials. All Cz samples were submitted to an initial short homogenisation step at 1050 °C for 15 min.

Processing

Wafers have been subjected to certain solar cell processing steps to simulate the thermal load during cell fabrication. The applied processing steps are visualized in figure 2. After the annealing steps described in figure 1 (only for Cz wafers), a $POCl_3$ diffusion in an open-tube furnace was carried out leading to an emitter sheet resistivity of 50 Ω/sq. PECVD SiN deposition was performed in a remote plasma reactor using ND_3 instead of NH_3. The SiH_4 to ND_3 ratio was 1/1.6 resulting in a refractive index n of 2.1-2.2. The following firing step in a conventional belt furnace was the same as used for co-firing of screen-printed metal contacts in industrial-type solar cell processing.

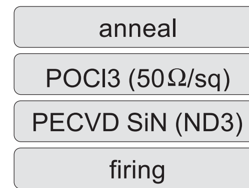

Figure 2: Processing steps applied to all samples shown in tables 1 and 2.

Afterwards samples have been investigated using FTIR and SIMS. Instead of H we detected D to reduce the signal-to-noise ratio. To reduce SIMS measurement time, samples have been beveled as shown in figure 3. The combination of several measurements along the surface of the bevel results in depth profiles. The depths can easily be calculated from the bevel angle (2.5°).

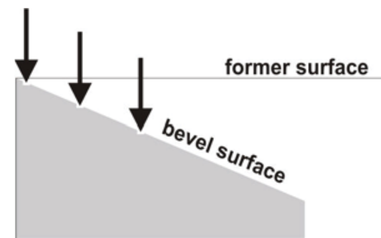

Figure 3: Beveling of samples for convenient determination of profiles using SIMS.

RESULTS

Material 1 - RGS

Results for the RGS samples listed in table 1 after bevelling can be seen in figure 4 (see [4,5] for more details on this study). D-profiles after PECVD deposition and firing could be measured by SIMS for samples RGS1, RGS2, and RGS3. A high [O] leads to high [D] near the surface (RGS1) and a steeper profile (RGS1 as compared to RGS3). Sample RGS1 with a higher as-grown [O_i] leads to a slightly steeper D-profile compared to sample RGS2 with the same overall [O] but lower as-grown [O_i].

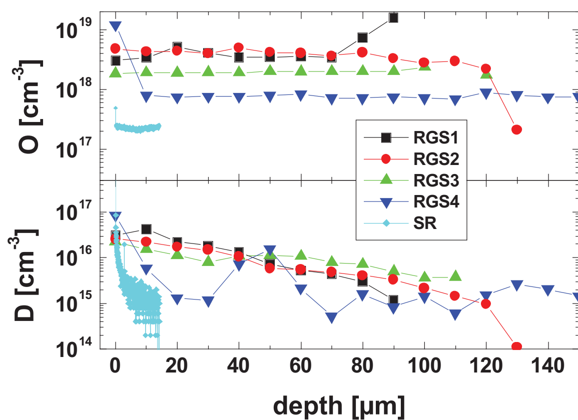

Figure 4: SIMS profiles of [O] and [D] for the RGS samples shown in table 1 with String Ribbon as a low [O] reference.

Samples RGS4 and SR with [O] <10^{18} cm^{-3} lead to [D] in the range of the detection SIMS limit (around 10^{15} cm^{-3} for these measurements). The hump at 40-50 µm depth for sample RGS4 coincides with a grain boundary, indicating that D might be trapped at the defects present near the grain boundary. The SR sample was not bevelled.

It is known that H or D interacts with O-precipitates, reducing their recombination activity. Therefore, it was concluded in [4,5] that D-profiles are only detectable in mc Si provided O is present in sufficient concentrations. In addition it could be shown that vacancy concentration [vac] is strongly affected by the high temperature steps during wafer fabrication and sample processing. As [vac] was suggested to play an important part in diffusion kinetics of H in Si [8] we concluded that for the RGS samples under investigation [vac] did not play the most important role. This was deduced from the fact that samples RGS1 and RGS2 differ strongly in [vac] but show very similar D-profiles [4,5].

Furthermore, in [4] it was stated that interaction between D and O might take place via the interface of the O-precipitates formed at high temperatures. This would explain why there is a slightly steeper D-profile for RGS1 compared to RGS2 with the same overall [O] but a large amount of small O-precipitates in RGS1 and a smaller amount of larger O-precipitates in RGS2. This speculation can only be investigated in more detail when another material is chosen, which allows investigation of this specific feature.

Material 2 - Cz

Annealing of the different Cz materials resulted in O-precipitation as indicated in table 2. Densities of O-precipitates after Anneal 1 are estimated to be 10^{14} cm^{-3} for Cz1 and 10^{12} cm^{-3} for Cz2. For Anneal 2 they are estimated to be 10^{11} cm^{-3} for Cz1 and 10^{9} cm^{-3} for Cz2. If trapping of D is due to interaction with the surface of the O-precipitate as suggested in [4], we would expect to observe the highest [D] for Cz1 after Anneal 1 with lots of small precipitates having the highest surface-to-volume ratio.

SIMS results for the samples presented in table 2 are shown in figure 5. Here not the complete D-profiles are displayed but only values from the top (SiN layer) and the bottom (no SiN layer) of the wafer. The SIMS detection limit for this experiment was around $5 \cdot 10^{14}$ cm^{-3}.

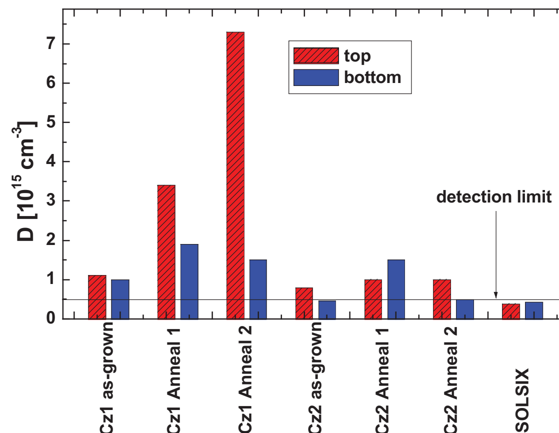

Figure 5: D-concentration for samples listed in table 2. Given are values at the top (SiN) and bottom side of the samples.

Higher D-signals can be seen for Cz1 samples with higher overall [O], as expected. This indicates once again that high [O] leads to more trapping of D. Note that for the SOLSIX sample [D] is close or below the SIMS detection limit as it was observed in [9].
Surprisingly, the highest [D] can be detected for Cz1 after Anneal 2 leading to large O-precipitates in lower concentration than for Anneal 1. This clearly contradicts to the assumption that the amount of D-atoms trapped in the vicinity of O-precipitates increases only with the surface-to-volume ratio of the O-precipitates as it was proposed in [4]. To further investigate this behavior, D-profiles have been measured on beveled samples from Cz1 material. These results are shown in figure 6.

Lowest [D] can be detected for sample Cz1 as grown. Sample Cz1 Anneal 1 shows higher [D]. As there is no difference in the overall [O] (samples originating from the same Cz wafer), we have to conclude that trapping of D is influenced by the way O is present. Here it is obvious that the formation of a large amount of small precipitates (density estimated to be 10^{14} cm^{-3}) leads to more trapping of D. As the amount of precipitates is large enough to detect more than one precipitate during the SIMS scan (30x30 µm scan size with a beam size of 100 µm), the resulting D-profile is quite smooth.

Things are different for sample Cz1 Anneal 2. Here we detect the highest D-signal although the overall surface area of the O-precipitates is lower compared to sample Cz1 Anneal 1. An explanation for more trapping of D in this sample could be that interaction of D and the O-precipitate does not take place only via the surface of the

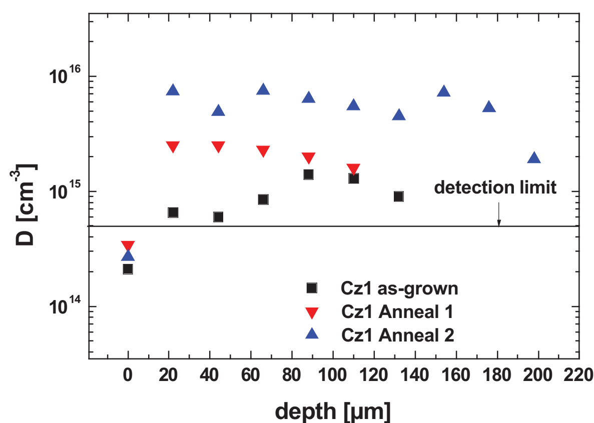

Figure 6: SIMS profiles of [D] for the Cz1 samples shown in table 2.

precipitate but due to the strain field around it. Larger precipitates might produce more stress in their vicinity and therefore more D-atoms can be trapped to relax chemical bonds between Si atoms. This of course does not mean that there is no direct interaction possible between D and the precipitate or its surface (or even oxygen on interstitial lattice site). It just gives an additional location for trapping.

Data for Cz1 Anneal 2 has more scatter as compared to Cz1 Anneal 1. This could be due to the fact that the number of O-precipitates being hit by the SIMS detection beam is much smaller (in the range of 10 assuming a depth resolution of 10 nm), causing a more scattered signal.

Interestingly, all data points close to the initial wafer surface show significantly lower [D]. This could be explained by out-diffusion of O during the annealing steps. As this drop in D-signal can be detected even for Cz1 as-grown, this out-diffusion should happen already at the initial homogenisation step at 1000 °C for 15 min, which was applied for all Cz samples.

SUMMARY

It could be shown that the amount of hydrogen (or in this case deuterium) trapped in crystalline Si is strongly dependant on the concentration of O present in the material. Two experiments carried out on mc RGS material and mono-crystalline Cz material clearly revealed the influence of O on trapping of D for both materials.

In the first experiment four RGS wafers differing in [O] and the way O was precipitated have been chosen. Pronounced SIMS signals and steep D-profiles indicating effective trapping could be detected only for RGS material with [O] well above 10^{18} cm^{-3}. Lower [O] material led to SIMS signals in the range of the detection limit. In RGS material with [O] well below 10^{18} cm^{-3} effective hydrogenation can be achieved in significantly shorter passivation times and at lower temperatures, leading to higher minority carrier lifetimes [7,10].

For the second experiment two Cz materials differing in as-grown [O] have been investigated. To study the influence of O-precipitation on trapping of D, these samples were submitted to two thermal annealing steps producing O-precipitates of different sizes and concentrations. Highest SIMS signals are detected for the high [O] Cz sample showing large O-precipitates. This clearly indicates that interaction of D with O-precipitates is not restricted to the surface of the precipitate, as lower SIMS signals have been detected in the sample with smaller precipitates in higher concentration showing a higher overall surface area.

The results presented in this study may lead to better hydrogenation techniques in solar cell processing for O-rich cost-effective mc Si materials.

ACKNOWLEDGEMENTS

Parts of this work have been funded by the EC within the RGSells project (ENK6-CT2001-00574) and the German BMU in the frame of the ASIS project (0329846J).

LITERATURE

[1] A. Van Wieringen, N. Warmoltz, Physica **22**, 1956, 849

[2] M. Stavola, F. Jiang, A. Rohatgi, D. Kim, J. Holt, H. Atwater, J.P. Kalejs, Proc. 3rd WC PEC, Osaka 2003, 909

[3] M. Stavola, in Properties of Crystalline Si, edited by R. Hull (INSPEC, London, 1999), 511

[4] G. Hahn, D. Sontag, S. Seren, A. Schönecker, A.R. Burgers, R. Ginige, K. Cherkaoui, D. Karg, H. Charifi, Proc. 19th EC PVSEC, Paris 2004, 427

[5] D. Karg, H. Charifi, G. Pensl, M. Schulz, G. Hahn, Proc. 19th EC PVSEC, Paris 2004, 709

[6] H. Lange, I.A. Schwirtlich, *J. Crystal Growth* **104**, 1990, 108

[7] S. Seren, G. Hahn, A. Gutjahr, A.R. Burgers, A. Schönecker, this conference

[8] B.L. Sopori, X. Deng, J.P. Benner, A. Rohatgi, P. Sana, S.K. Estreicher, Y.K. Park, M.A. Roberson, *Solar Energy Materials & Solar Cells* **41/42**, 1996, 159

[9] H.F.W. Dekkers, S. De Wolf, G. Agostinelli, J. Szlufcik, T. Pernau, W.M Arnoldbik, H.D. Goldbach, R.E.I. Schropp, Proc. 3rd WC PEC, Osaka 2003, 983

[10] G. Hahn, A. Schönecker, J. Phys.: Condens. Matter 16, 2004, R1615